NASA Technical Memorandum 4573

Automatic Computation of Euler-Marching and Subsonic Grids for Wing-Fuselage Configurations

Raymond L. Barger and Mary S. Adams
Langley Research Center • Hampton, Virginia

Ramki R. Krishnan
Analytical Services & Materials, Inc. • Hampton, Virginia

July 1994

Introduction

The problem of generating grids for flow calculations over airplane configurations is important because the grid represents the object on which the flow code operates. Several sophisticated procedures have been developed for generating grids for fairly complex configurations from specifications read in from the screen by interactive methods. (See ref. 1.) However, such hands-on interactive methods are too time-consuming to be feasible when geometries must be modified frequently and automatically, as in optimal design calculations. Many trade-off studies can be performed without the complete detailed airplane geometry, as for example, wing-fuselage or wing-fuselage-fin configurations. For such simplified configurations, great generality in grid-generation techniques is not required and simpler procedures that can be automated become appropriate.

The purpose of this paper is to describe one such automatic grid-generation procedure. The algebraic method used is a variant and generalization of the method of transfinite interpolation. Examples of its application to generating an Euler-marching grid and a grid for subsonic flow calculation are provided.

Symbols

$\mathcal{A}$	cross-section aspect ratio
i, j, k	indices for ξ, η, ζ grid surfaces, respectively
p	input parameter to control χ
q	superellipticity exponent (eqs. (3) and (4))
r	radius of grid outer boundary
$\mathbf{r}$	two-dimensional position vector with components y, z
s	arc length
x, y, z	Cartesian coordinates (longitudinal, lateral, and vertical body axis, respectively)
$\bar{z}$	z location of symmetry line for superellipse
α, γ, δ	blending functions
θ	superellipse angle parameter
λ	scaling function
ξ, η, ζ	grid coordinates
ρ	superellipse scale parameter
χ	superellipse eccentricity parameter
ψ	variable defined by equation (8)

Subscripts:

g	generic grid point
i	inner
max	maximum value
n	nondimensionalized quantity
o	outer boundary
s	surface
u	upstream grid limit

Procedure

The geometry input is normally in the wave-drag, or Harris, format. (See ref. 2.) This format describes the configuration as a set of separate components and is convenient for making changes in geometry parameters. The geometry is read into a program (ref. 3) that completes the geometry by computing the wing-fuselage and fin-fuselage intersection lines and that generates a surface grid. (See fig. 1.) To initiate the volume grid calculation, a new surface grid is computed by interpolating in the initial grid along $x =$ Constant lines. Then an outer boundary shape is specified, and the grid is generated by interpolation between the surface and this outer boundary. Details of this procedure follow.

Surface Grid

For the initial surface grid lines, points are distributed along $x =$ Constant cuts on the fuselage ahead of the wing. In the wing region, the wing lofting lines are extended to the fuselage surface by the method of reference 3 and then are continued around the fuselage along $x =$ Constant lines. (See fig. 2.)

Now, a new surface grid is computed by interpolating in the original grid at $x =$ Constant stations. Because the grid is already laid out this way on the fuselage, the interpolation there involves only the x variable. On the wing, the interpolation is a matter of locating where the lofting lines intersect the $x =$ Constant planes.

Care must be taken in distributing the points on these lines so that grid continuity is ensured. The main problem locations are at the wing and fin leading and trailing edges. The grid variable in the circumferential direction at $x =$ Constant is denoted η. (See fig. 3.) To prevent the constant-η surface lines from running from the lower to the upper surface or vice versa, the entire configuration is treated as separate upper and lower surfaces. Thus, each $x =$ Constant line consists of two distinct segments, one on the upper surface and the other on the lower surface. In the wing region the break is taken

at the wing tip. On the fuselage ahead of the wing, it is taken at the same angular location as the point where the wing leading edge intersects the fuselage. (See fig. 3.) This system ensures grid continuity in the η direction at the wing leading edge.

Grid points are distributed along each of the upper and lower surface $x = $ Constant lines as a function of arc length. The arc is initiated at the $y = 0$ point, and the cumulative arc length s is computed at successive points out to the break point. This procedure enables us to express the grid points on the line as functions of s (i.e., $y(s), z(s)$). Then this distribution of points can be replaced through interpolation by any desired distribution. At present this distribution function is specified by a cubic polynomial with arbitrary coefficients to permit flexibility in designing the surface grid. To ensure continuity in the longitudinal direction, this distribution is specified globally so that if, for example, the points are congested near the wing tips, they will also be congested on the fuselage ahead of the wing in the region that corresponds to the wing tips. An example of the resulting surface grid is shown in figure 4.

At the wing trailing edge a problem arises when the $x = $ Constant lines are interpolated from the initial surface grid. If the trailing edge is swept, a gap occurs between the intersection of an $x = $ Constant plane with the fuselage and its intersection with the wing. (See fig. 5.) This problem is treated by including the gap region as part of the surface grid (fig. 6) but labeling the grid points in this region as wake points. To maintain continuity, the wake is assumed to intersect the fuselage at the same angular location as the wing trailing edge. A vertical fin would be treated similarly if present.

Volume Grid

After the surface grid has been established, the individual two-dimensional grid surfaces for an Euler-marching grid are generated by specifying a corresponding distribution of points on an appropriate outer boundary line and then interpolating between the surface points and outer boundary points. An appropriate outer boundary shape is a circle that lies slightly outside the Mach cone whose vertex is at or slightly ahead of the nose of the configuration. If $\mathbf{r}_s$ denotes a vector representation of the cut through the body surface and $\mathbf{r}_o$ denotes the outer boundary shape, then a straightforward transfinite interpolation for the intermediate grid-line shapes (lines of constant ζ) would result from a variation of the form

$$\mathbf{r}_g = (1 - \alpha)\mathbf{r}_s + \alpha\mathbf{r}_o \qquad (1)$$

where α is a blending, or homotopy, function of ζ that varies continuously and monotonically from 0 to 1.

For this type of grid the skewness can be severe, as is illustrated in figure 7. Somewhat better control over the grid shape can be realized by the method of reference 4. The inner and outer boundary shapes are nondimensionalized, thereby reducing them to the same scale. Then the homotopy function can be used to establish a pure shape variation, whereas the scaling is specified by an independent function $\lambda(\zeta)$. Thus,

$$\mathbf{r}_g = \lambda[(1 - \alpha)\mathbf{r}_{ns} + \alpha\mathbf{r}_{no}] \qquad (2)$$

However, for difficult shapes such as that shown in figure 7, this generalization is not sufficient. The radial ($\eta = $ Constant) grid lines near the wing-fuselage juncture need a larger $|y|$ component to be more nearly normal at the body surface. This effect could be accomplished by replacing the circular outer boundary with a highly eccentric ellipse. However, an eccentric ellipse would not be appropriate for flow calculation, and it would not help the problem at the wing tips, where the $\eta = $ Constant lines require a larger z component to reduce the skewness.

An outer boundary shape that would reduce the skewness at both the wing tips and the wing-fuselage juncture is a superellipse, which is defined by

$$y = \chi\rho|\cos\theta|^q \text{sign}(\cos\theta) \qquad (3)$$

$$z = \rho|\sin\theta|^q \text{sign}(\sin\theta) + \tilde{z} \qquad (4)$$

where χ is the eccentricity parameter and q is the superellipticity exponent. This outer boundary shape does reduce the skewness at the body surface, but it does not yield a practical grid away from the surface. However, this problem can be overcome by making a further generalization of the transfinite interpolation formula. Returning to equation (1), we replace the fixed circular outer boundary shape $\mathbf{r}_o$ with a function that varies parametrically with ζ such that it becomes a circle at the largest value of ζ. At small values of ζ (near the surface), $\mathbf{r}_o$ becomes the superellipse of equation (3). Between these two extremes, $\mathbf{r}_o$ is defined as a smooth blend of the inner function $\mathbf{r}_{io}$ and the outer function $\mathbf{r}_{oo}$ by a homotopy function $\gamma(\zeta)$:

$$\mathbf{r}_o = (1 - \gamma)\mathbf{r}_{io} + \gamma\mathbf{r}_{oo} \qquad (5)$$

This function replaces $\mathbf{r}_o$ in equation (1).

In equation (3), both the eccentricity parameter χ and the superellipticity exponent q are specified in terms of the cross-section aspect ratio $\mathcal{A} = y_{max}/$Fuselage semiheight. Thus,

$$\chi = 1 + p\left(\frac{\mathcal{A} - 1}{\mathcal{A} + 1}\right) \tag{6}$$

where p is an adjustable input parameter of the order of 1 and

$$q(\zeta) = \psi + (1 - \psi)\gamma(\zeta) \tag{7}$$

where the variable

$$\psi = \frac{1}{\chi^2} \tag{8}$$

Also in equation (4) the z symmetry line $z = \bar{z}$ is taken where the superellipse is intersected by a line drawn from the fuselage center through the wing tip.

Thus, near the surface, the influence of r_o on the grid shape is that of a superellipse, but far from the surface it becomes that of a circle. This effect is seen in the example shown in figure 8.

Several typical surfaces of the complete three-dimensional grid are shown in figure 9. Figure 10 shows results of an Euler flow calculation on this grid. The marching procedure used for this calculation is similar to that of reference 5. For the half plane $y \geq 0$, the grid dimensions are 97, 97, and 49 in the ξ, η, and ζ directions, respectively.

Subsonic Grid

A grid for calculating subsonic flows over a configuration must extend well ahead of, behind, and to the sides of the configuration. One type of subsonic grid can be generated starting with the same techniques used to generate the Euler grid but by changing the outer boundary shape from a cone to a more appropriate shape. Then, the two-dimensional surfaces at $x =$ Constant cuts are changed into three-dimensional surfaces by distorting them out of the $x =$ Constant planes.

An example has been calculated for which the outer boundary is taken to be a semiellipsoid upstream that is connected to a cylinder downstream at the x station for which the wing attains its maximum span. (See fig. 9(a).) The radius distribution of the ellipsoid is

$$r = r_{max}\sqrt{1 - \left[\frac{(x - x_s)}{(x_u - x_s)}\right]^2} \tag{9}$$

where x_u is the grid station that is farthest upstream. The radius of the downstream cylinder is, of course,

$$r = r_{max} \tag{10}$$

The two-dimensional $x =$ Constant grid surfaces are converted to three-dimensional surfaces by supplementing equation (2) with an x variation

$$x_g = (1 - \delta)x_s + \delta x_o \tag{11}$$

where the subscript g is the generic grid point and δ is a homotopy function. Typical surfaces of this grid are shown in figure 11.

Concluding Remarks

Several procedures for the automatic generation of flow computation grids for relatively simple configurations have been described. For supersonic flows, a quasi-two-dimensional grid for marching Euler codes was developed, and some sample results in graphical form were included. For subsonic flows, the procedure was modified by distorting the $x =$ Constant grid surfaces out of plane and by specifying a more appropriate outer boundary shape. The techniques are algebraic and are based on a generalization of the transfinite interpolation method.

References

1. Smith, Robert E., ed.: *Software Systems for Surface Modeling and Grid Generation.* NASA CP-3143, 1992.

2. Middleton, W. D.; Lundry, J. L.; and Coleman, R. G.: *System for Aerodynamic Design and Analysis of Supersonic Aircraft. Part 2- User's Manual.* NASA CR-3352, 1980.

3. Barger, Raymond L.; and Adams, Mary S.: *Automatic Computation of Wing-Fuselage Intersection Lines and Fillet Inserts With Fixed-Area Constraint.* NASA TM-4406, 1993.

4. Barger, Raymond L.; and Adams, Mary S.: *Semianalytic Modeling of Aerodynamic Shapes.* NASA TP-2413, 1985.

5. Morrison, J. H.; and Korte, J. J.: Implementation of Vigneron's Streamwise Pressure Gradient Approximation in Parabolized Navier-Stokes Equations. *AIAA J.*, vol. 30, no. 11, Nov. 1992, pp. 2774-2776.
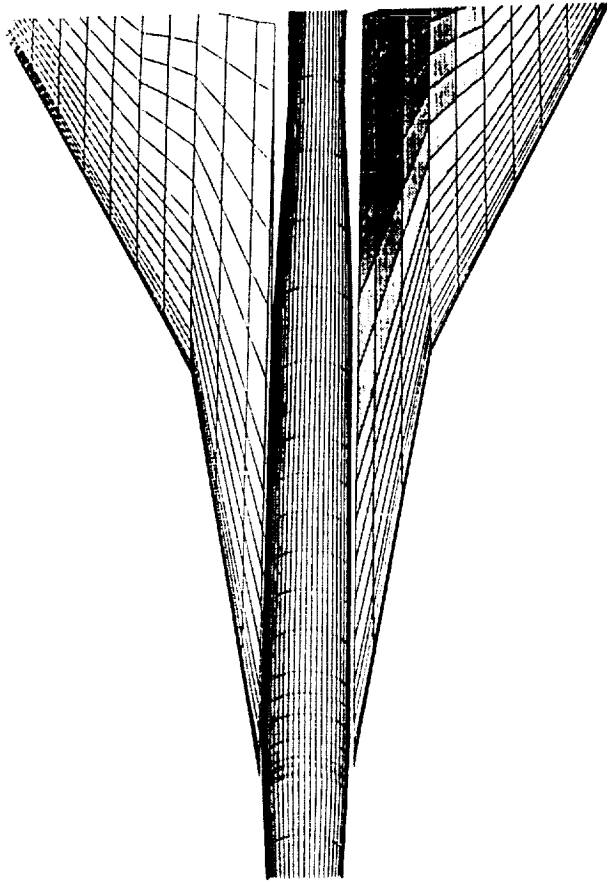
(a) Original configuration (from wave-drag data).
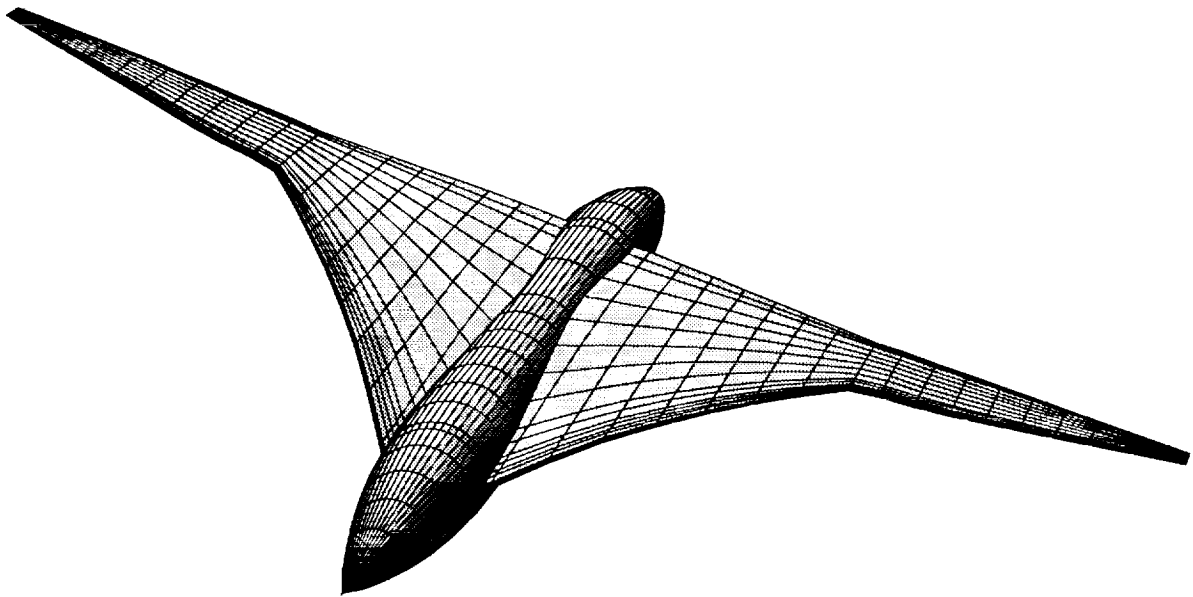
(b) Configuration with computed intersection line (lower surface).

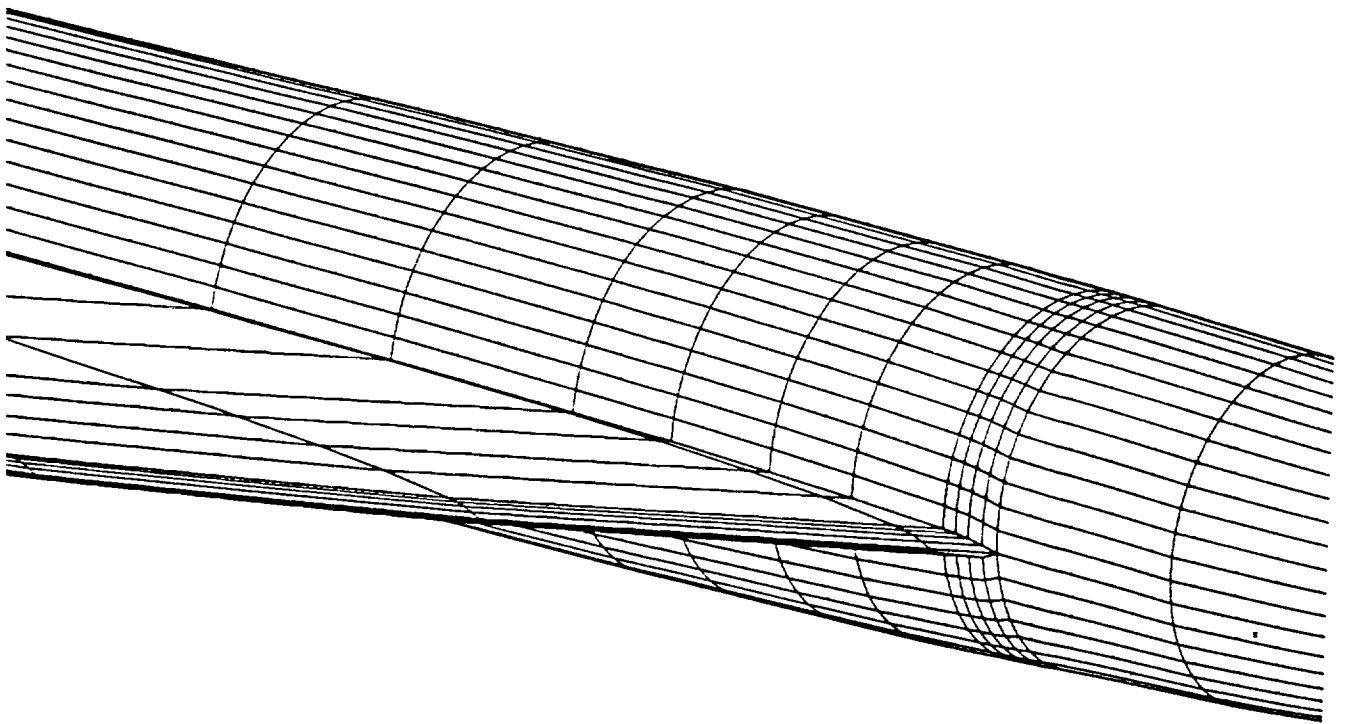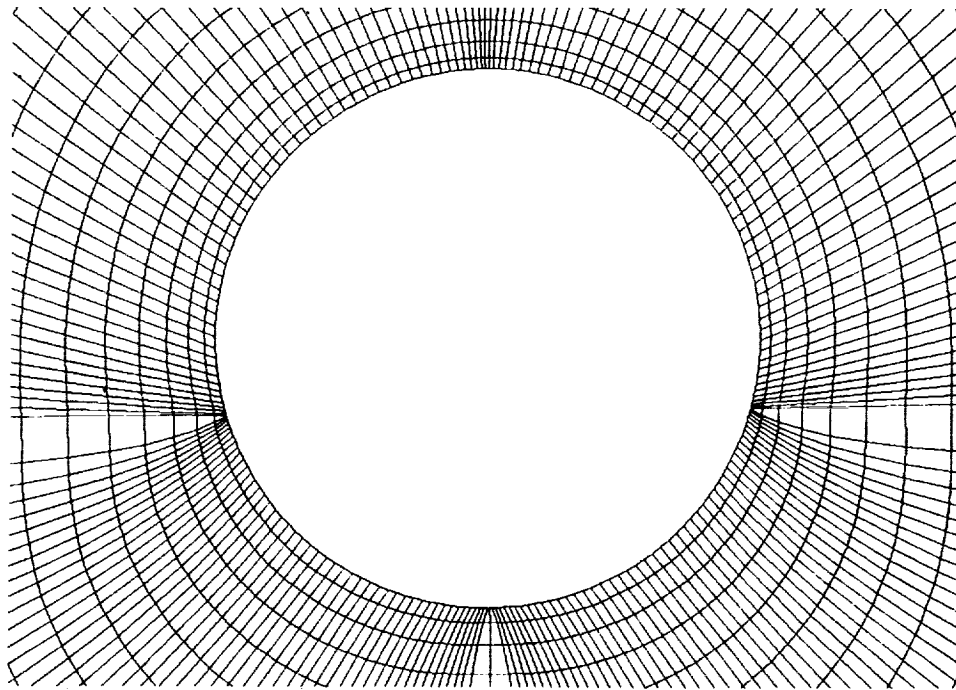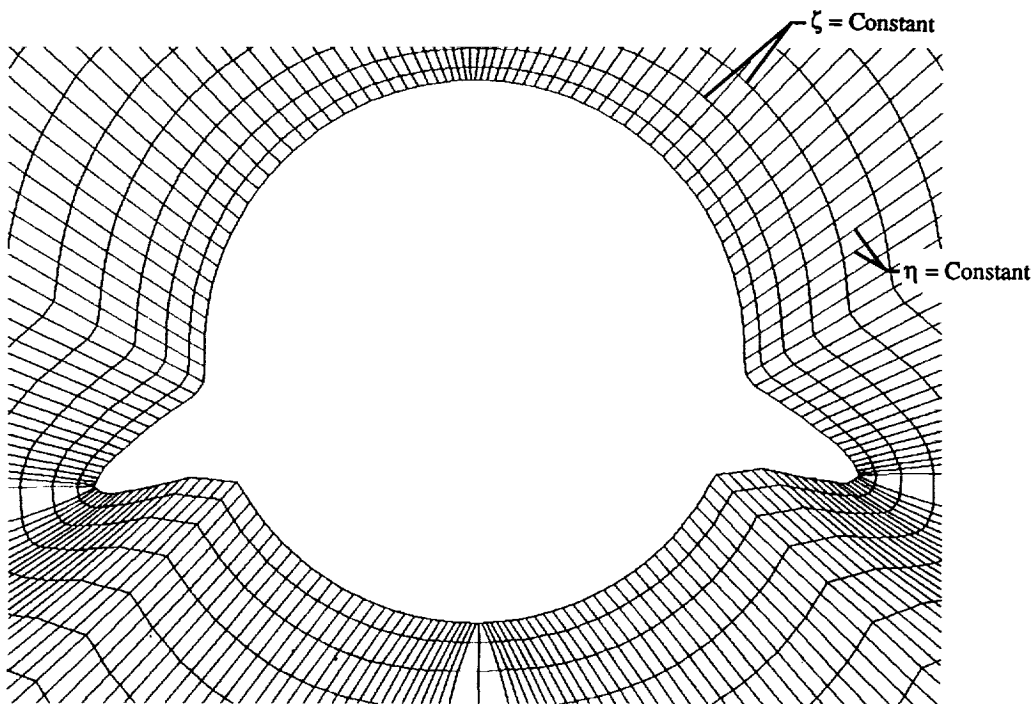Figure 1. Calculated wing-fuselage intersection.

Figure 2. Close-up view of intersection line and surface grid near wing leading edge.

(a) Grid section ahead of wing leading edge intersection with fuselage.

ζ = Constant

η = Constant

(b) Grid section behind wing leading edge intersection with fuselage.

Figure 3. Grid sections displaying grid coordinates and circumferential distribution of grid lines.
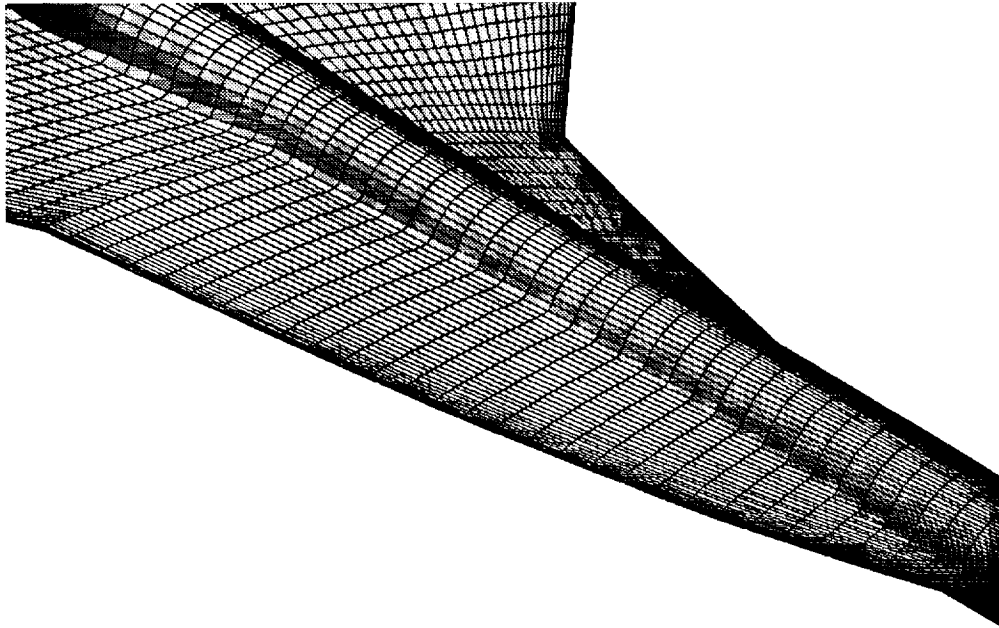
Figure 4. Revised surface grid to initialize Euler-marching grid. $x = $ Constant lincs are computed by interpolating in original grid and redistributing points.

Gap between fuselage
and swept wing
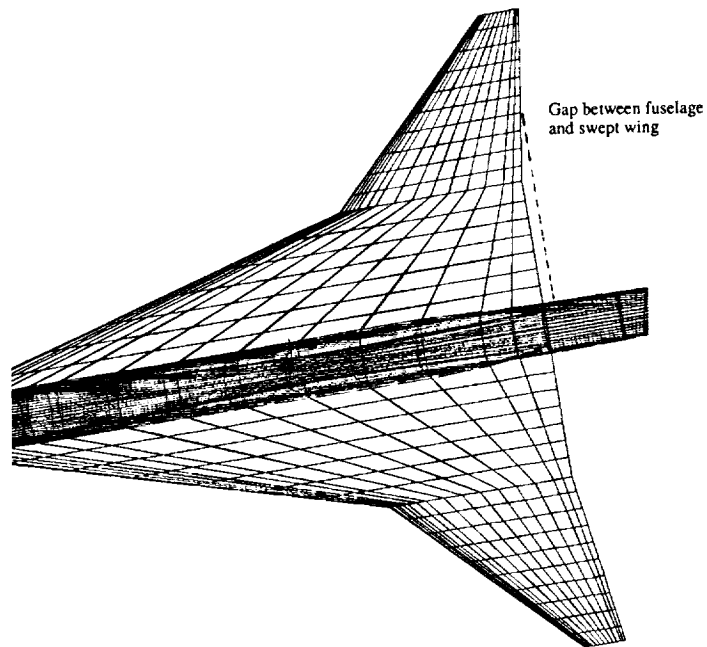
Figure 5. Plan view illustrating gap that occurs in $x = $ Constant grid line when trailing edge is swept.
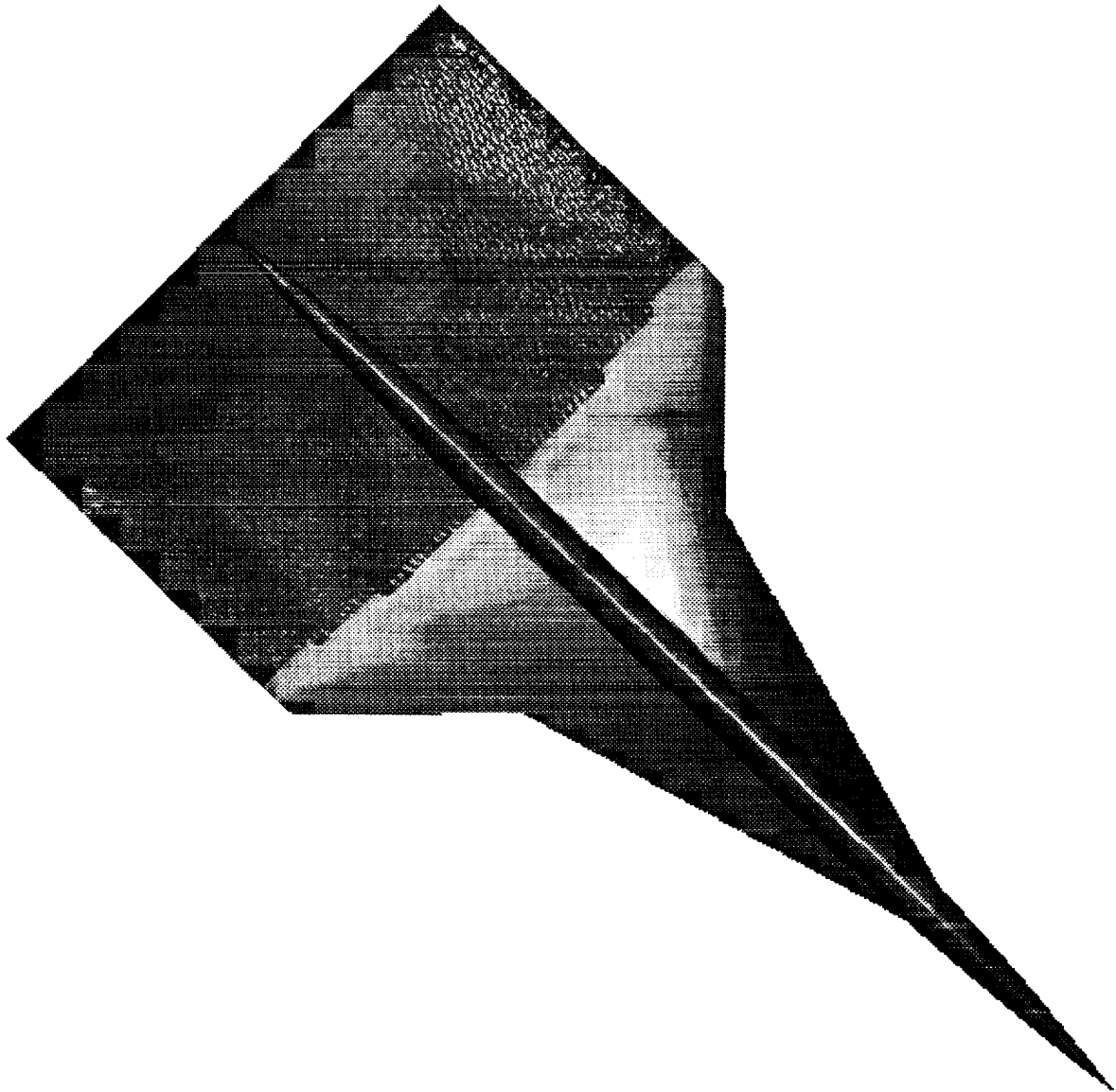
Figure 6. Plan view of configuration with wake.
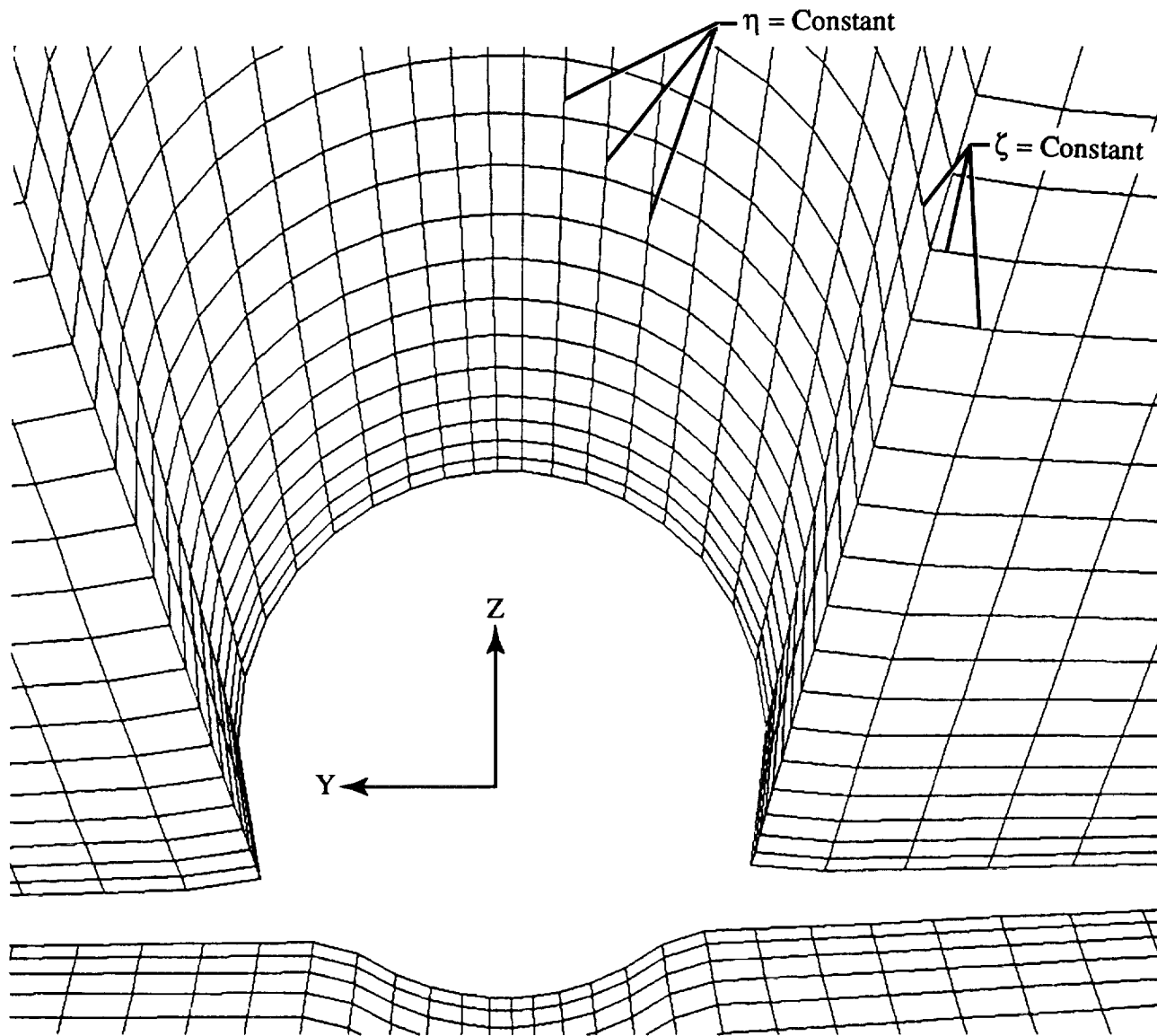
(a) Wing-body juncture region.
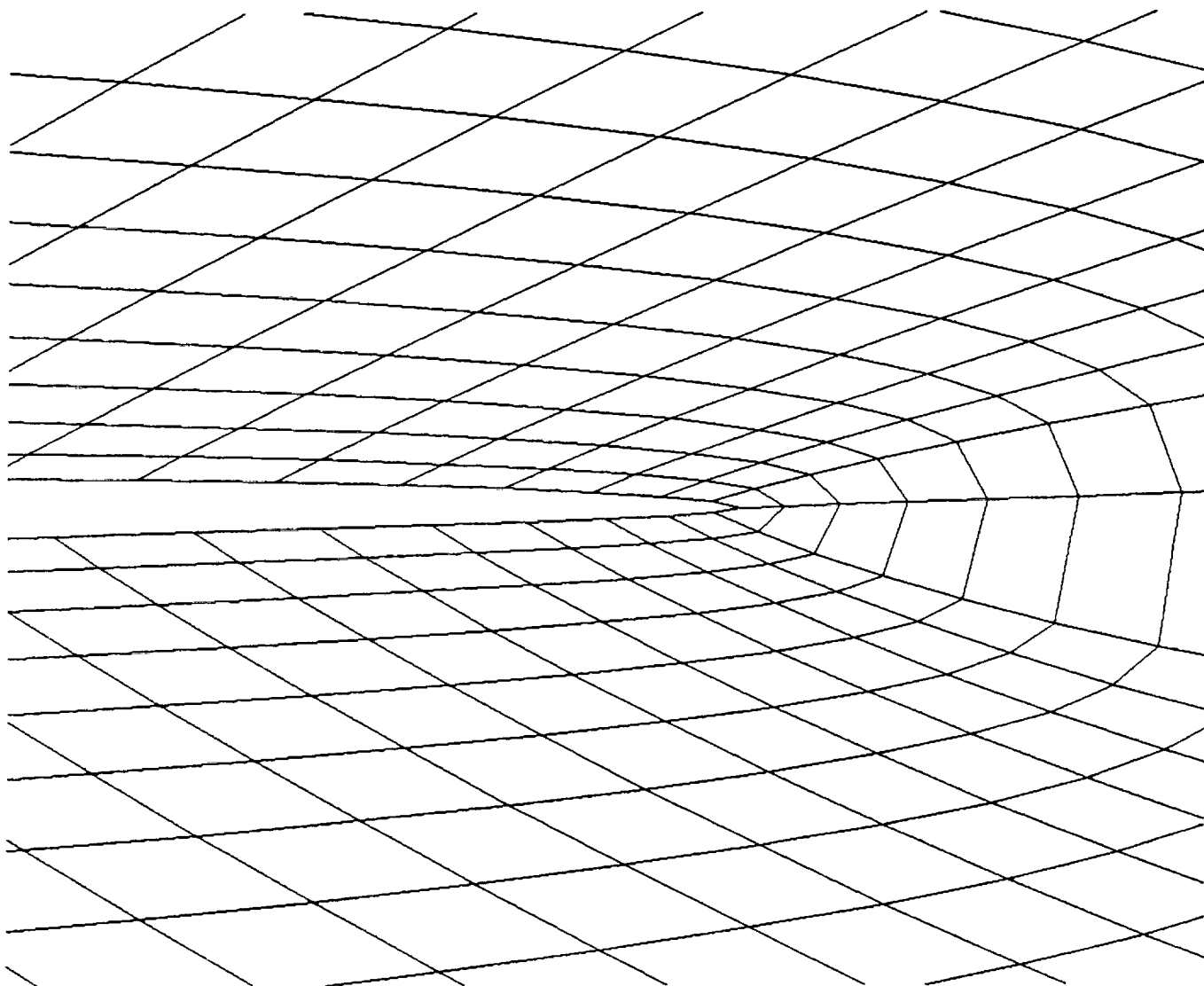
Figure 7. Grid skewness problem at body surface.
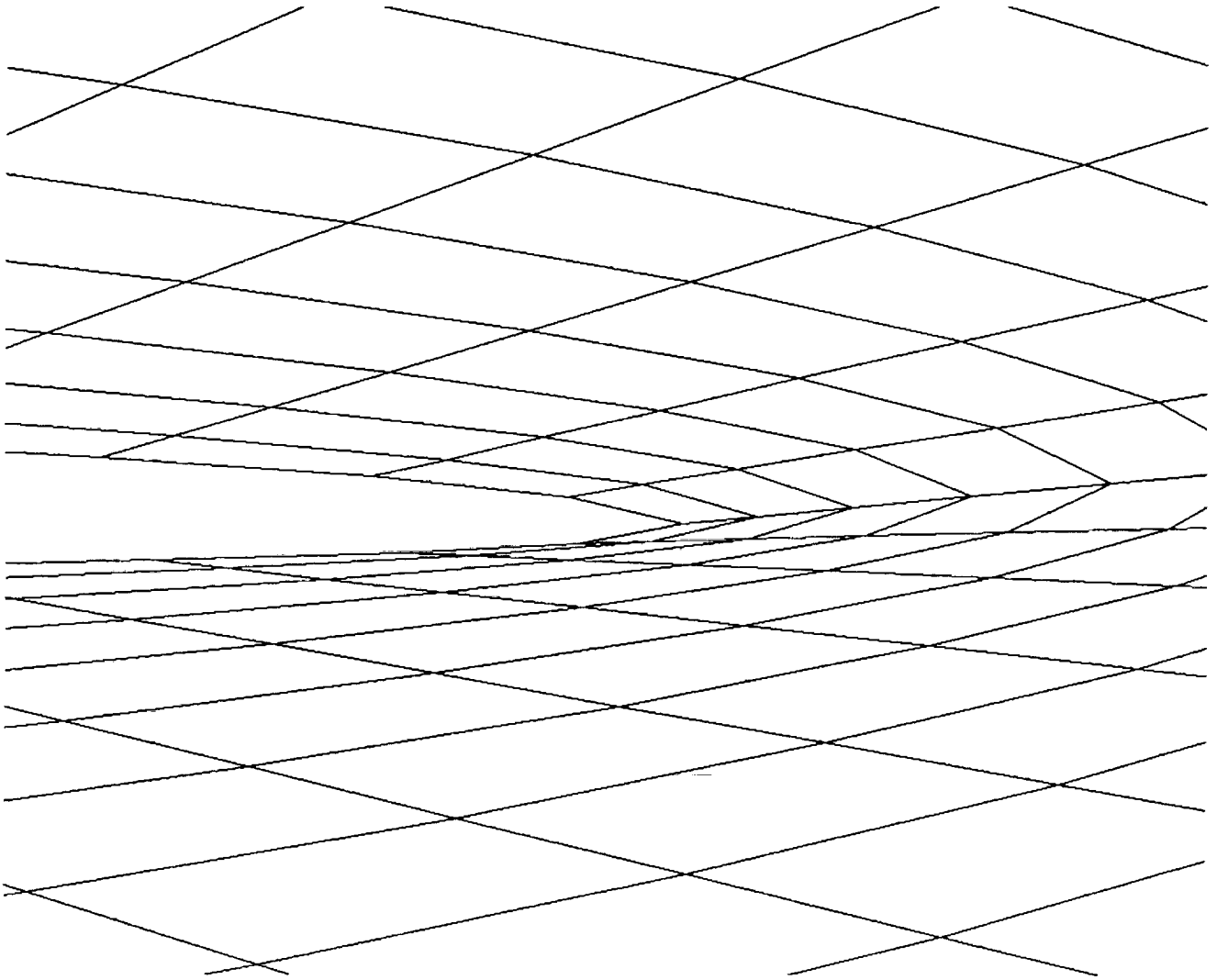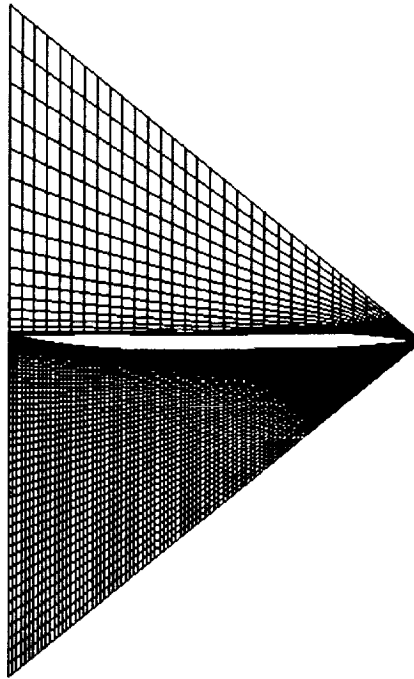
(b) Wing-tip region.

Figure 7. Concluded.
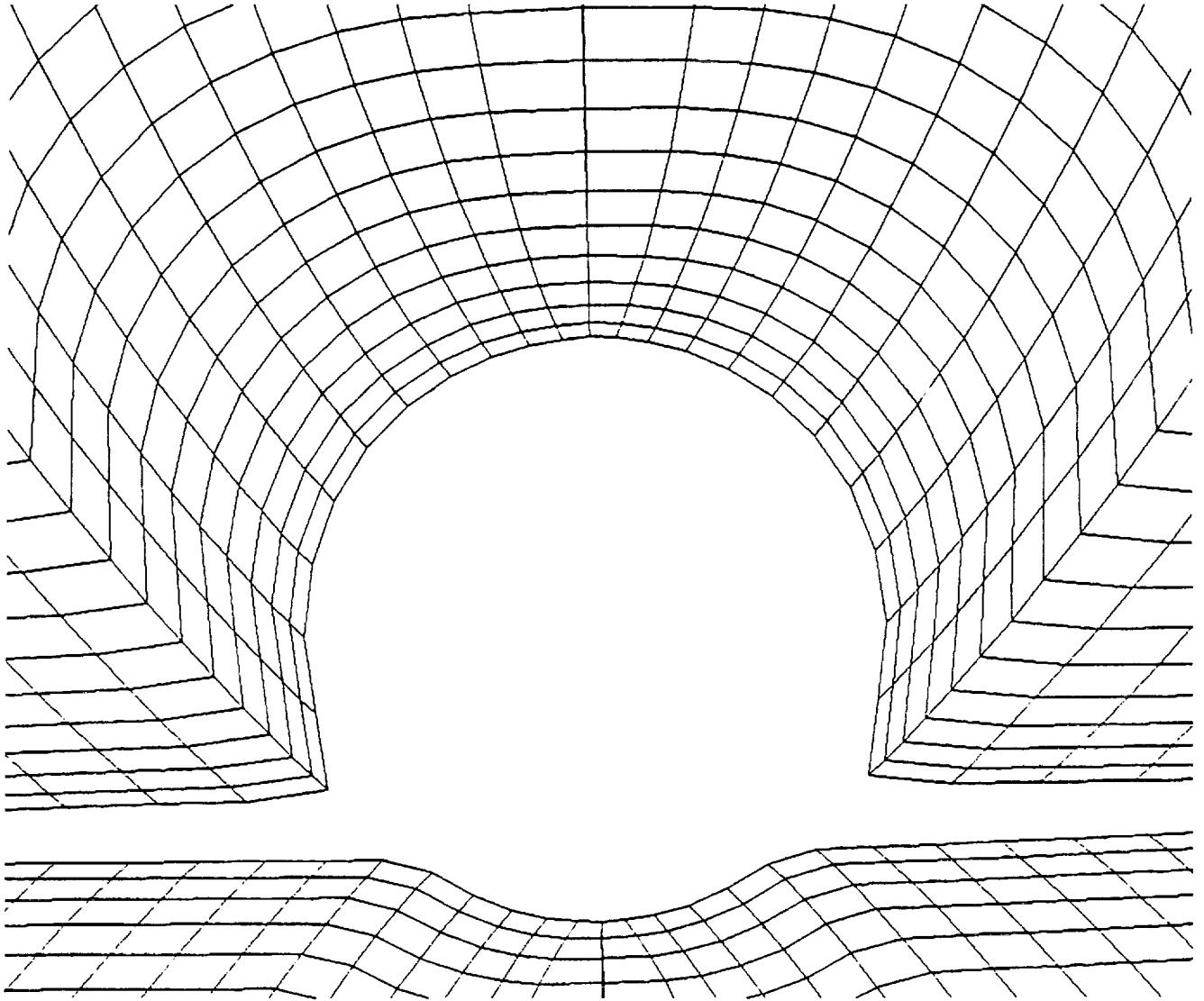
(a) Wing-body juncture region.

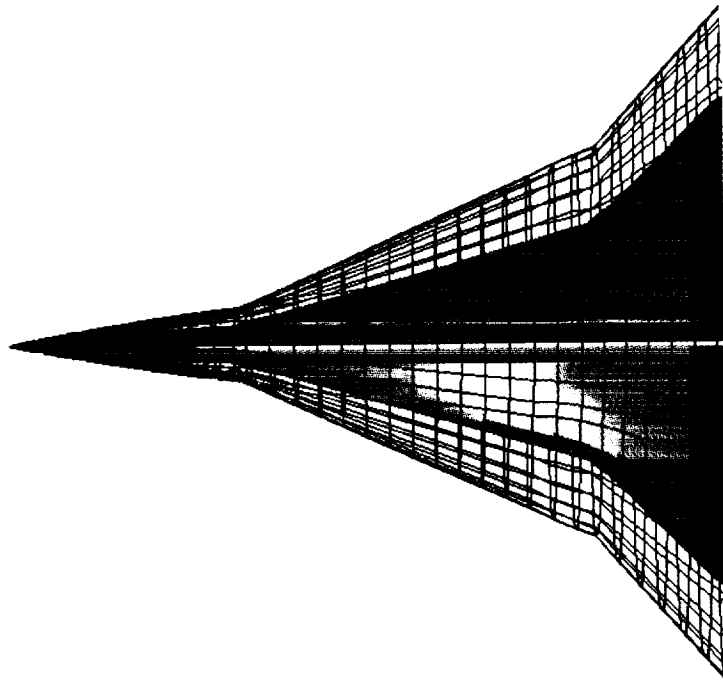Figure 8. Grid skewness reduction at body surface.

(b) Wing-tip region.

Figure 8. Concluded.

(a) $j = 1$ and 97 surfaces (upper grid surface diluted to improve clarity).

(b) $k = 12$ surface (grid diluted to improve clarity).

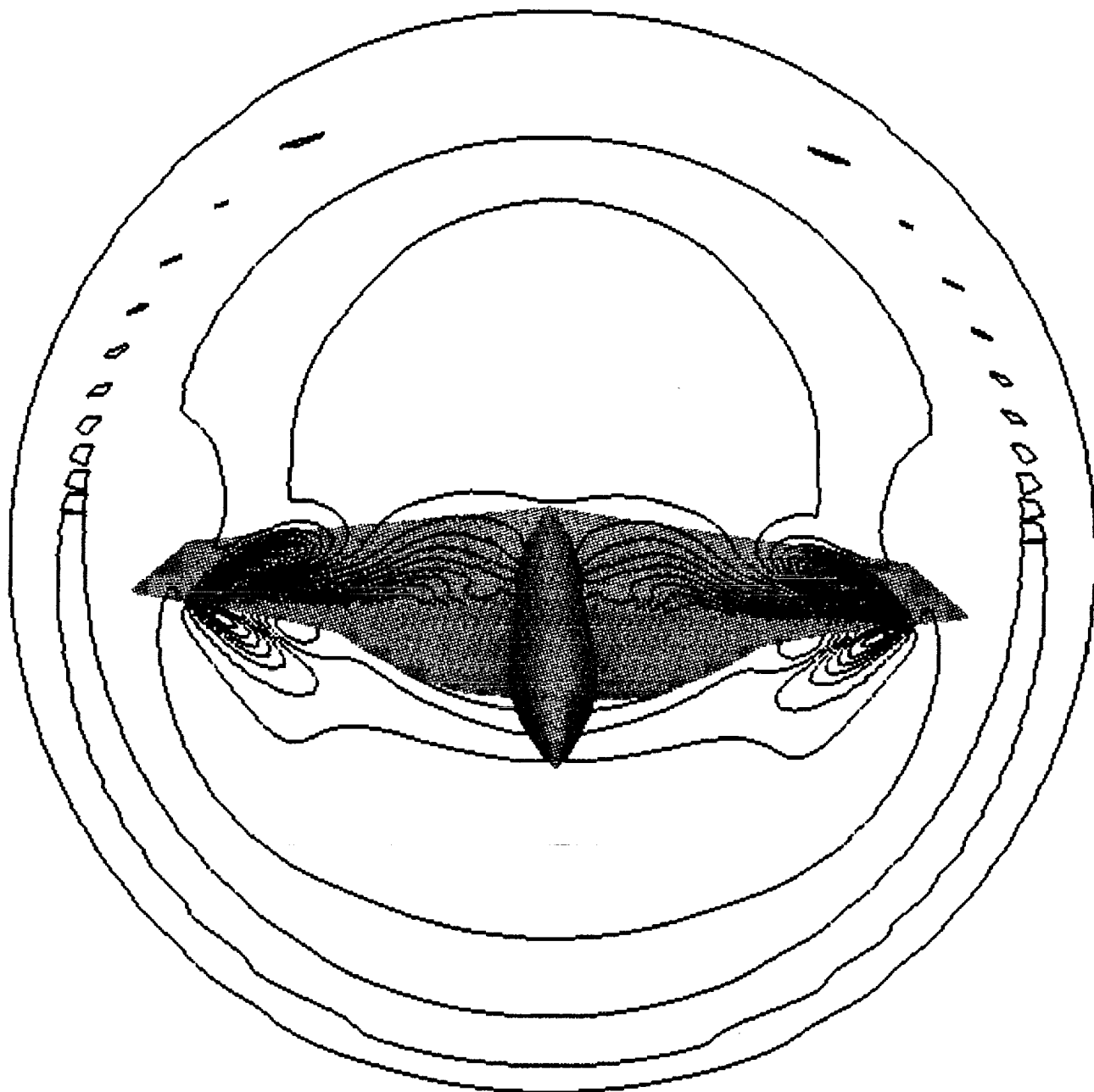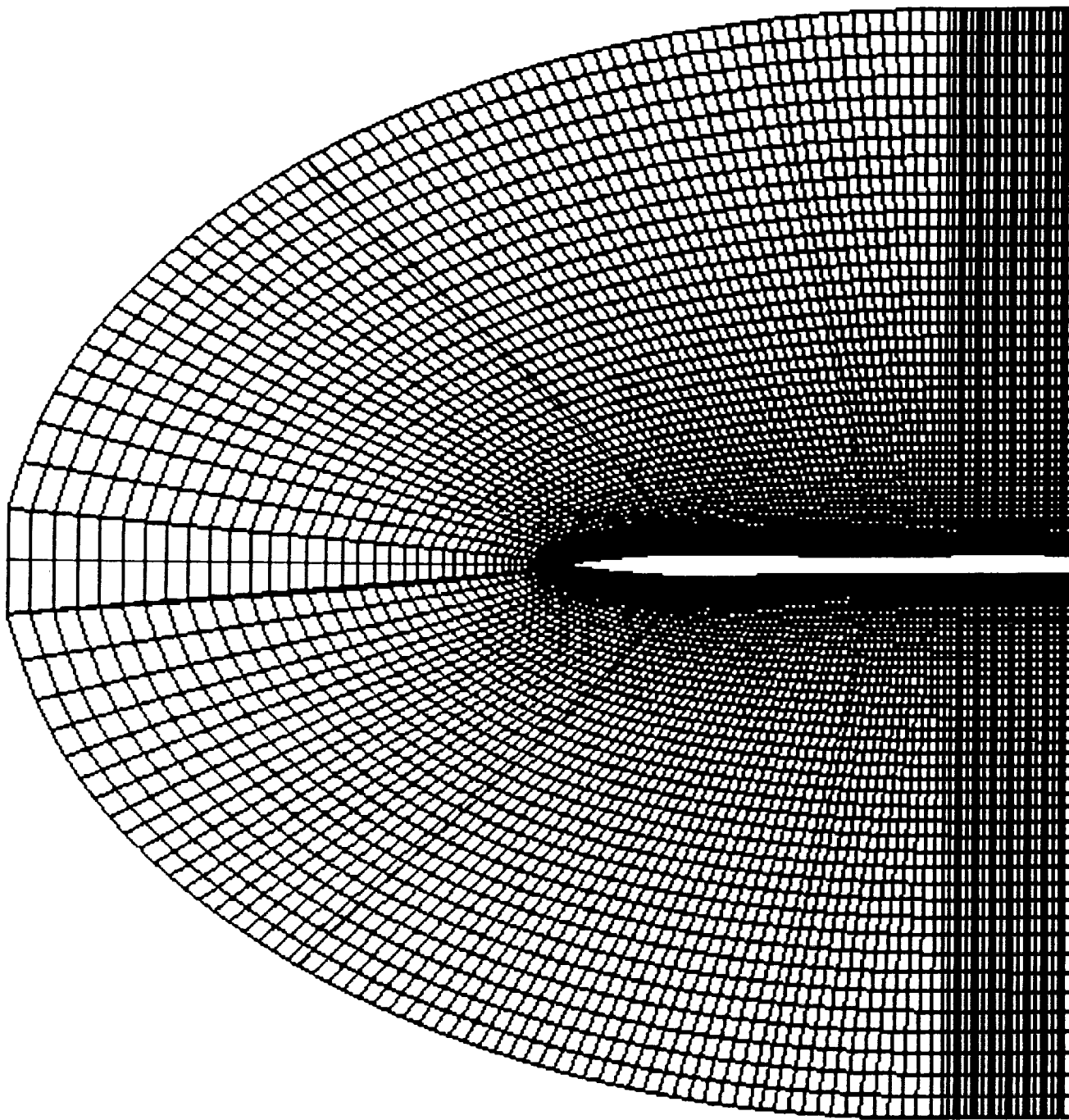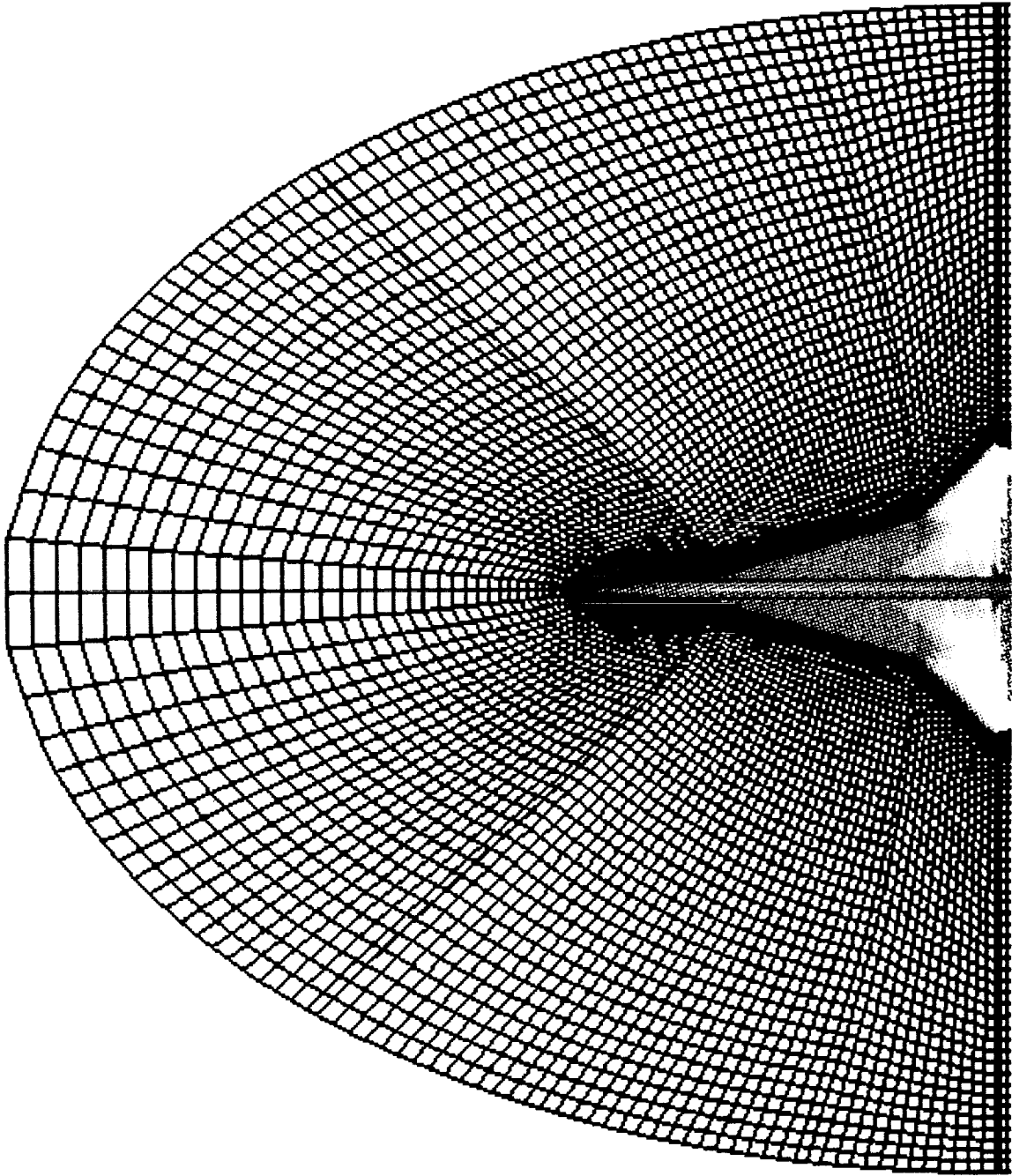Figure 9. Typical surfaces of Euler-marching grid.

13

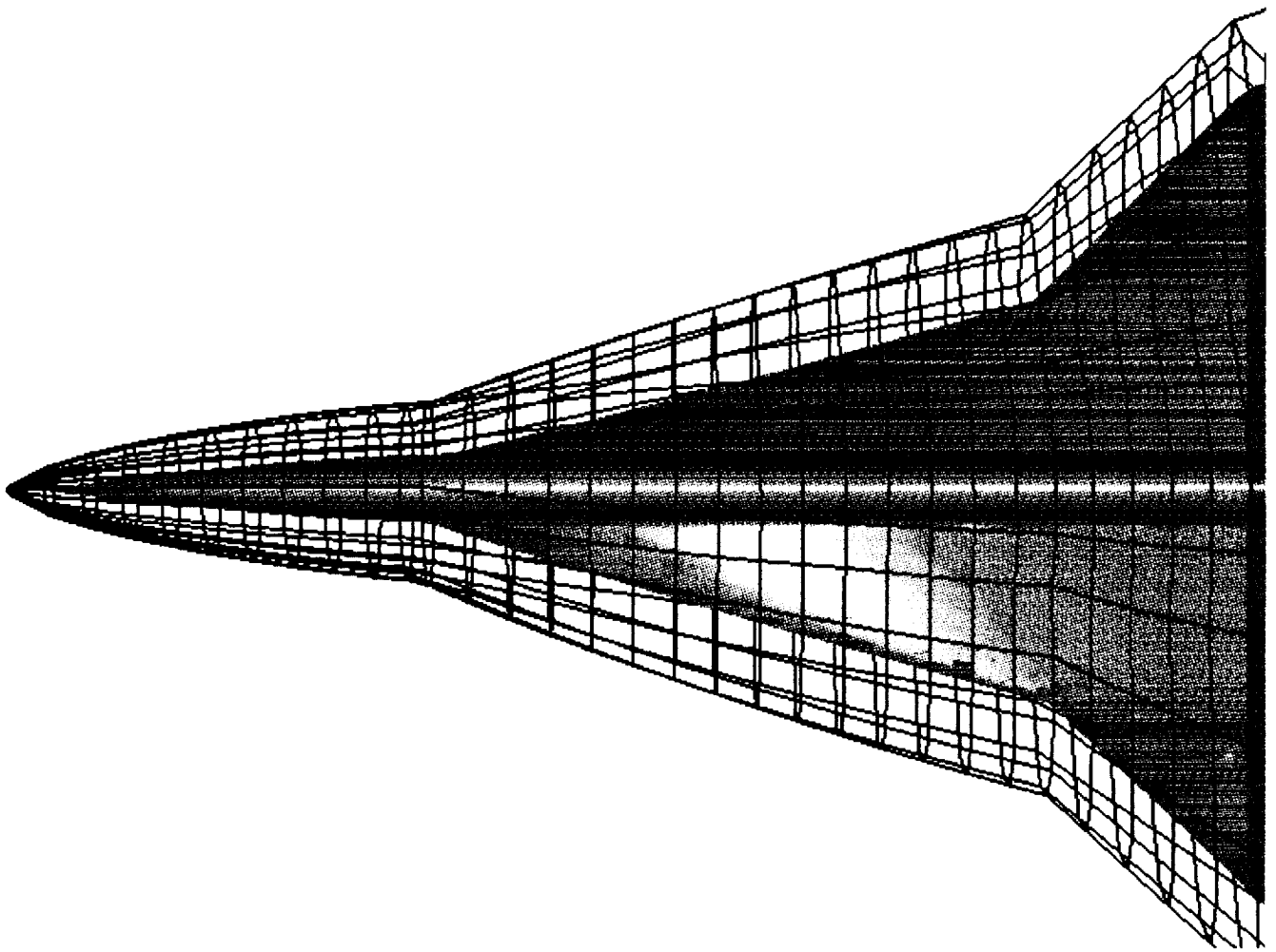Figure 10. Euler-marching flow solution; pressure contours at $x = 97$ station.

(a) $j = 1$ and 97 surfaces.

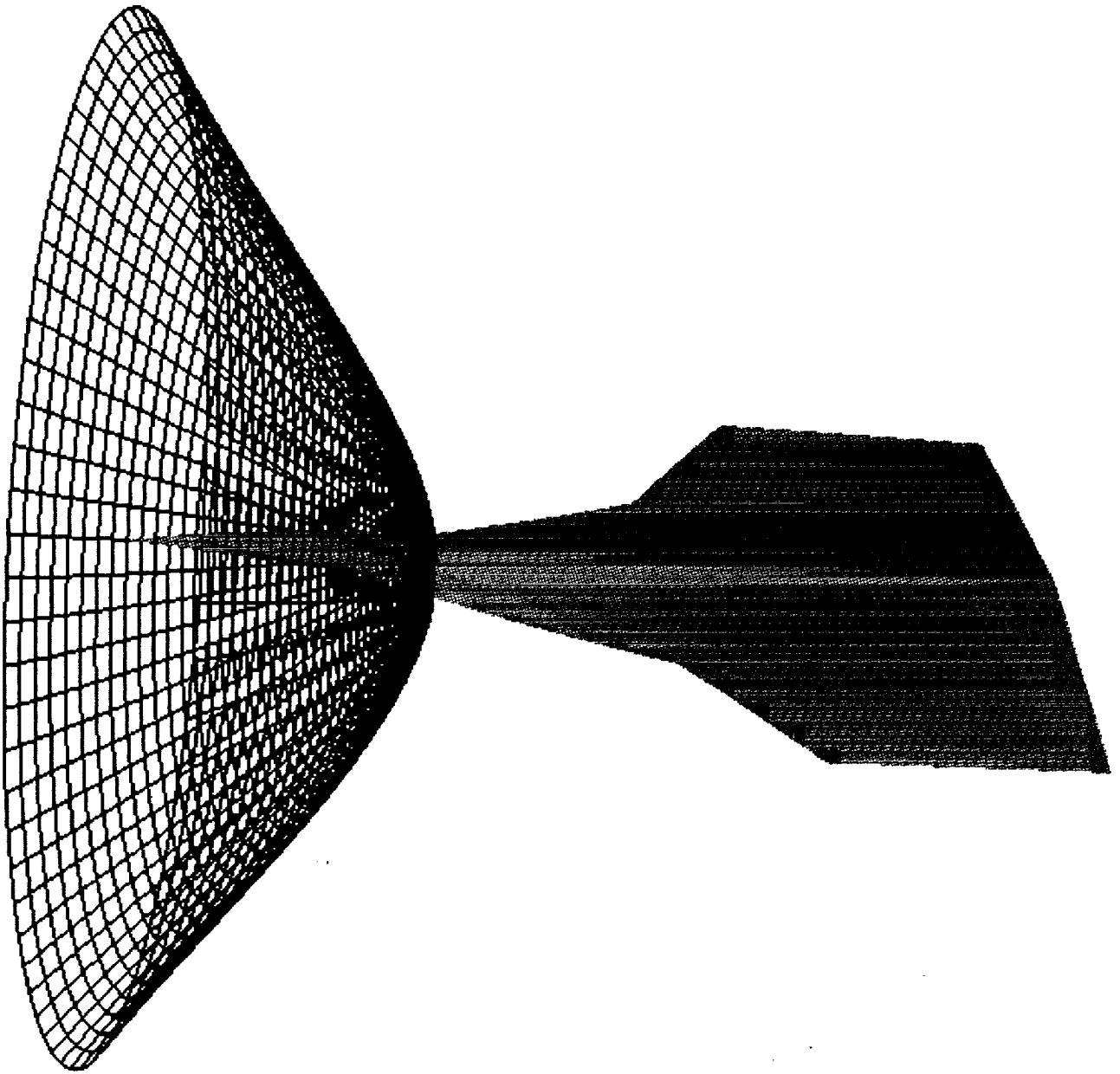Figure 11. Typical surfaces of subsonic flow grid.

(b) $j = 49$ surface.

Figure 11. Continued.

(c) $k = 12$ surface (grid diluted to improve clarity).

Figure 11. Continued.

(d) $i = 24$ surface.

Figure 11. Concluded.

.

REPORT DOCUMENTATION PAGE

Public reporting burden for this collection of information is estimated to average 1 hour per response, including the time for reviewing instructions, searching existing data sources, gathering and maintaining the data needed, and completing and reviewing the collection of information. Send comments regarding this burden estimate or any other aspect of this collection of information, including suggestions for reducing this burden, to Washington Headquarters Services, Directorate for Information Operations and Reports, 1215 Jefferson Davis Highway, Suite 1204, Arlington, VA 22202-4302, and to the Office of Management and Budget, Paperwork Reduction Project (0704-0188), Washington, DC 20503.

1. AGENCY USE ONLY(Leave blank)	2. REPORT DATE July 1994	3. REPORT TYPE AND DATES COVERED Technical Memorandum

4. TITLE AND SUBTITLE Automatic Computation of Euler-Marching and Subsonic Grids for Wing-Fuselage Configurations	5. FUNDING NUMBERS WU 509-10-11-01
6. AUTHOR(S) Raymond L. Barger, Mary S. Adams, and Ramki R. Krishnan	

7. PERFORMING ORGANIZATION NAME(S) AND ADDRESS(ES) NASA Langley Research Center Hampton, VA 23681-0001	8. PERFORMING ORGANIZATION REPORT NUMBER L-17364

9. SPONSORING/MONITORING AGENCY NAME(S) AND ADDRESS(ES) National Aeronautics and Space Administration Washington, DC 20546-0001	10. SPONSORING/MONITORING AGENCY REPORT NUMBER NASA TM-4573

11. SUPPLEMENTARY NOTES

Barger and Adams: Langley Research Center, Hampton, VA; Krishnan: Analytical Services & Materials, Inc., Hampton, VA.

12a. DISTRIBUTION/AVAILABILITY STATEMENT Unclassified–Unlimited Subject Category 02	12b. DISTRIBUTION CODE

13. ABSTRACT *(Maximum 200 words)*

Algebraic procedures are described for the automatic generation of structured, single-block flow computation grids for relatively simple configurations (wing, fuselage, and fin). For supersonic flows, a quasi-two-dimensional grid for Euler-marching codes is developed, and some sample results in graphical form are included. A type of grid for subsonic flow calculation is also described. The techniques are algebraic and are based on a generalization of the method of transfinite interpolation.

14. SUBJECT TERMS Grid generation; Automatic procedures; Aircraft geometry	15. NUMBER OF PAGES 19
	16. PRICE CODE A03

17. SECURITY CLASSIFICATION OF REPORT Unclassified	18. SECURITY CLASSIFICATION OF THIS PAGE Unclassified	19. SECURITY CLASSIFICATION OF ABSTRACT Unclassified	20. LIMITATION OF ABSTRACT